



HAL
open science

First test of a Li₂WO₄(Mo) bolometric detector for the measurement of coherent neutrino-nucleus scattering

A Aliane, I.Ch Avetissov, O.P Barinova, X de la Broise, F.A Danevich, L Dumoulin, L Dussopt, A Giuliani, V Goudon, S.V Kirsanova, et al.

► To cite this version:

A Aliane, I.Ch Avetissov, O.P Barinova, X de la Broise, F.A Danevich, et al.. First test of a Li₂WO₄(Mo) bolometric detector for the measurement of coherent neutrino-nucleus scattering. Nuclear Instruments and Methods in Physics Research Section A: Accelerators, Spectrometers, Detectors and Associated Equipment, 2020, 949, pp.162784. 10.1016/j.nima.2019.162784 . hal-02423673

HAL Id: hal-02423673

<https://hal.science/hal-02423673v1>

Submitted on 20 Jul 2022

HAL is a multi-disciplinary open access archive for the deposit and dissemination of scientific research documents, whether they are published or not. The documents may come from teaching and research institutions in France or abroad, or from public or private research centers.

L'archive ouverte pluridisciplinaire **HAL**, est destinée au dépôt et à la diffusion de documents scientifiques de niveau recherche, publiés ou non, émanant des établissements d'enseignement et de recherche français ou étrangers, des laboratoires publics ou privés.



Distributed under a Creative Commons Attribution - NonCommercial 4.0 International License

First test of a $\text{Li}_2\text{WO}_4(\text{Mo})$ bolometric detector for the measurement of coherent neutrino-nucleus scattering

A. Aliane^a, I. Ch. Avetissov^b, O.P. Barinova^b, X. de la Broise^c,
F.A. Danevich^d, L. Dumoulin^e, L. Dussopt^a, A. Giuliani^{e,f}, V. Goudon^a,
S.V. Kirsanova^b, T. Lasserre^c, M. Loidl^g, P. de Marcillac^e, S. Marnieros^e,
C. Nones^{c,*}, V. Novati^e, E. Olivieri^e, D.V. Poda^{d,e}, T. Redon^e, M. Rodrigues^g,
V.I. Tretyak^d, M. Vivier^c, V. Wagner^c, A.S. Zolotarova^{c,e}

^aCEA/LETI MINATEC, 17 Avenue des Martyrs, 38054 Grenoble, France

^bDmitry Mendeleev University of Chemical Technology of Russia, Miusskaya sq. 9, 125047 Moscow, Russia

^cIRFU, CEA, Université Paris-Saclay, 91191 Gif-sur-Yvette, France

^dInstitute for Nuclear Research, 03028 Kyiv, Ukraine

^eCSNSM, Univ. Paris-Sud, CNRS/IN2P3, Université Paris-Saclay, 91405 Orsay, France

^fDISAT, Università dell'Insubria, 22100 Como, Italy

^gCEA, LIST, Laboratoire National Henri Becquerel, 91191 Gif-sur-Yvette, France

Abstract

The first observation of coherent elastic neutrino-nucleus scattering ($\text{CE}\nu\text{NS}$), reported by the COHERENT Collaboration in 2017, paved the way for a new generation of experiments using reactor $\bar{\nu}_e$ and aiming at precisely measuring this process. In this context, the BASKET (Bolometers At Sub-KeV Energy Thresholds) R&D project investigates the use of cryogenic detectors for a reactor $\text{CE}\nu\text{NS}$ experiment. This article reports on the first test of a Mo-doped lithium tungstate scintillating bolometer ($\varnothing 18 \times 7$ mm, 8 g), performed in an aboveground laboratory at CSNSM, Orsay (France). The detector bolometric performance (energy and time response, particle identification capabilities) and radiopurity have been studied and confirm the promising potential of lithium tungstate-based bolometric detectors for the measurement of $\text{CE}\nu\text{NS}$ at reactors.

Keywords: Neutrino Physics, Coherent Elastic Neutrino-Nucleus Scattering, Low temperature detectors, Scintillating bolometers, Cryogenics

*Corresponding author

Email address: claudia.nones@cea.fr (C. Nones)

1. Introduction

The first observation of coherent elastic neutrino-nucleus scattering (CE ν NS) [1], reported in 2017 by the COHERENT Collaboration [2, 3], has recently renewed a great interest in precisely measuring this process [4] as it offers a new way to probe physics beyond the standard model [5, 6, 7] and nuclear structure [8]. This process, where a neutrino coherently scatters off all the nucleons within a target nucleus at low momentum transfers, can exhibit a cross section up to two orders of magnitude higher than the standard neutrino detection channels such as the inverse beta decay reaction or $\bar{\nu}_e e^- \rightarrow \bar{\nu}_e e^-$ scattering, making it possible to perform precision physics experiments with kg-scale detectors rather than the ton- or kiloton-scale detectors used nowadays.

The ongoing experimental efforts and proposals mostly focus on studying this process at nuclear reactors [9, 10, 11, 12, 13], which deliver copious amounts of $\bar{\nu}_e$ with energies in the MeV range. The nuclear recoils signing CE ν NS events are then expected to have energies in the 0.01–1 keV range, depending on the target nucleus. Accessing such a very low energy deposition regime with detection techniques relying on scintillation or ionization signals seems quite difficult, and a promising alternative is the use of bolometric detectors which have the potential to reach the lowest energies and fully exploit a CE ν NS signal [10, 11, 13, 14]. Nuclear power plant environments usually offer experimental sites with shallow overburdens, implying the use of fast detectors with high background rejection capabilities. For instance, neutrons originating from the interactions of atmospheric muons in materials surrounding the detection setup can be of particular importance because they produce nuclear recoils identical to those coming from CE ν NS.

With this in mind, a new R&D program called BASKET (Bolometers At Sub-KeV Energy Thresholds) [15] has started in 2017 and aims at the development of cryogenic detectors suited to the study of CE ν NS in above-ground conditions. A key idea of the project is the use of scintillating crystals containing

30 a heavy element to enhance the CE ν NS rate¹ and lithium (natural, with $\sim 8\%$
 of ${}^6\text{Li}$ [16], or enriched in ${}^6\text{Li}$, e.g. see [17]) to study and mitigate the neutron
 backgrounds exploiting the ${}^6\text{Li}(n, t)\alpha$ reaction². As demonstrated in several
 past studies [19, 20, 21, 22, 23, 24, 25, 26, 27], such Li-containing bolometers
 can exhibit excellent particle identification capabilities and can be well-suited
 35 for the spectroscopy of neutrons. A low energy threshold Li-containing bolomet-
 ric detector could thus offer several advantages in a detection setup dedicated
 to the study of CE ν NS at reactors, such as being used as a CE ν NS event detec-
 tor, as a neutron flux monitoring device and/or even as an active veto (see e.g.
 [13, 14]) possibly acting as a neutron-absorption “skin” for another cryogenic
 40 detector.

This article reports on the first test of a cryogenic detector using a Mo-doped
 lithium tungstate crystal ($\text{Li}_2\text{WO}_4(\text{Mo})$) as an absorber material. The choice
 of lithium tungstate comes from the fact that tungsten is the heaviest element
 suitable for scintillator production and does not contain long-lived radioisotopes
 45 harmful for the study of CE ν NS³. Also, knowing about the chemical affinity be-
 tween Mo and W, previous studies performed on lithium molybdate (Li_2MoO_4)
 crystals further motivated this choice as they demonstrated excellent bolometric
 performances as well as low levels of radioactive impurities [23, 24, 25]. Finally,
 successful attempts to grow $\text{Li}_2\text{WO}_4(\text{Mo})$ crystals were already reported in the
 50 literature [28]. Growth of lithium tungstate crystals requires doping by molyb-
 denum at the few % mass fraction level [28]. However, such a molybdenum
 doping is expected to have a negligible impact on the $\text{Li}_2\text{WO}_4(\text{Mo})$ crystal
 bolometric performances, firstly because of the above-mentioned chemical affin-
 ity between Mo and W, and secondly because of the results about investigations
 55 on the tungsten doping of zinc molybdate crystals [29].

¹The CE ν NS cross section roughly scales with N^2 , N being the number of neutrons in the target nucleus.

²In particular, the cross section for thermal neutron capture is ~ 1 kb [18].

³Indeed, radioisotopes of ${}^{210}\text{Pb}$ and ${}^{207}\text{Bi}$ disfavour the choice of lead and bismuth respectively.

The article is structured as follows. The detector assembly and operation are presented in Section 2. Section 3 describes the results of the cryogenic test, focusing on the bolometric performance characterization of $\text{Li}_2\text{WO}_4(\text{Mo})$, on the particle identification capabilities of the detector and on the crystal radiopurity. Finally, Section 4 is devoted to the conclusion and perspectives.

2. Detector assembly and operation

A picture of the tested $\text{Li}_2\text{WO}_4(\text{Mo})$ crystal is shown on the left panel of Fig. 1. The cylindrical element is colorless and has a mass of 8 g. It was cut from a $\text{Li}_2\text{Mo}_{0.08}\text{W}_{0.92}\text{O}_4$ crystal boule (with a size of $\varnothing 25 \times 100$ mm) grown in a platinum crucible along the main crystallographic axis by the Czochralski technique with a pulling rate of 4 mm/h and a rotating rate of 10 rpm from a stoichiometric mixture of Li_2CO_3 (99.99 wt%), 5 mol. % MoO_3 (99.98 wt%) and 95 mol. % WO_3 (99.98 wt%) [28].

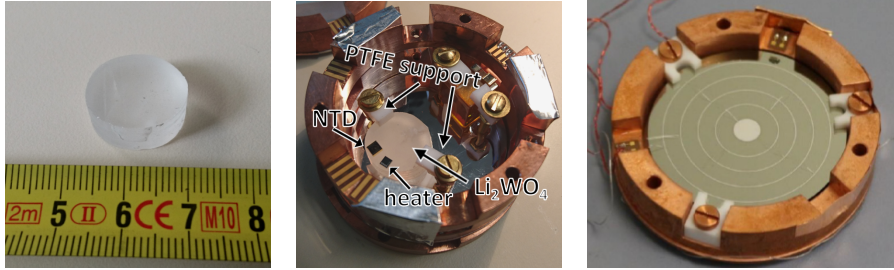


Figure 1: The $\text{Li}_2\text{WO}_4(\text{Mo})$ crystal sample with a size of $\varnothing 18 \times 7$ mm before (left) and after (center) its assembly used for the cryogenic test. The Cu holder was shared with another crystal (colored). A $\varnothing 44 \times 0.175$ mm Ge light detector (right), assisted with a Neganov-Trofimov-Luke signal amplification, was installed on the Cu housing top lid and faced the $\text{Li}_2\text{WO}_4(\text{Mo})$ bolometric detector to collect scintillation light.

The bolometric detector is shown on the middle panel of Fig. 1. A neutron transmutation doped (NTD) germanium thermistor [30] was used as a thermal sensor. It was directly glued on the crystal surface with a two-component epoxy glue (Araldite® Rapid). A P-doped silicon heater [31] was also glued on the same surface to inject periodically a constant power for an off-line stabilization

of the detector thermal response fluctuations [32]. The crystal was mounted and
75 fixed to a copper holder using PTFE supporting elements. Ultrasonic bondings
were used to connect the golden pads of the NTD to the gold-plated-on-Kapton
contacts glued on the holder with two Au wires ($\varnothing 25 \mu\text{m}$), providing both
thermal and electrical links, while the heater was bonded with two Al wires
($\varnothing 25 \mu\text{m}$). The $\text{Li}_2\text{WO}_4(\text{Mo})$ absorber was also equipped with a bolometric
80 light detector (LD) in order to measure emitted scintillation light and to study
particle identification using a dual readout technique (e.g., see [33] and references
therein). As shown by the right panel of Fig. 1, the LD consists of a thin
germanium slab ($\varnothing 44 \times 0.175 \text{ mm}$) with Al concentric electrodes deposited on
the surface. By applying an electric field, the bolometric signal originating from
85 the creation of electron-hole pairs can be amplified thanks to the Neganov-
Trofimov-Luke effect (see details in [34]). Finally, the internal bottom part of
the Cu housing was covered by a reflecting film (Enhanced Specular Reflector,
3M VikuitiTM) to improve the light collection.

The cryogenic test of the $\text{Li}_2\text{WO}_4(\text{Mo})$ crystal was performed above ground
90 at the CSNSM laboratory (Orsay, France) using a pulse-tube cryostat [35]
shielded by a lateral lead wall with 10-cm minimum thickness. A smeared
 ^{210}Po alpha source (made by ^{218}Po implantation into a copper substrate) was
used and placed on the copper holder approximately 1 cm away from the crystal
lateral surface. The crystal holder temperature was stabilized at 20 mK. The
95 NTD of the $\text{Li}_2\text{WO}_4(\text{Mo})$ detector was biased with a 6.25 nA current resulting
in a $0.6 \text{ M}\Omega$ working resistance; the operational point was chosen to get the best
signal-to-noise ratio. A room temperature DC-polarized electronics, developed
for the CUORICINO experiment [36], was placed inside a Faraday cage and
used for the readout of the channels. An active low-pass Bessel filter with a 675
100 Hz cut-off frequency was also used in the electronics chain. The LD electrode
bias was set either to 0 V or 23 V. The data, acquired in a stream mode, were
recorded by a 16-bit ADC (National Instruments NI USB-6218 BNC) with a 5
kHz sampling rate. Reference signals were injected by a pulse generator through
the heater every minute. The data were processed using an optimum filter tech-

105 nique [37]. The results of the data analysis are presented and discussed in the next section.

3. Results of the low-temperature test

The goal of the low temperature test of the $\text{Li}_2\text{WO}_4(\text{Mo})$ detector was to study its bolometric response, the energy resolution, the particle identification 110 capabilities and the radioactive contamination. Such information helps to evaluate the potential of this material to be used in a cryogenic $\text{CE}\nu\text{NS}$ experiment. The achieved results are detailed and discussed below.

3.1. Bolometric performances

The time profiles of the $\text{Li}_2\text{WO}_4(\text{Mo})$ and Ge LD signals are compared in 115 Fig. 2. The rising edge of the $\text{Li}_2\text{WO}_4(\text{Mo})$ pulse (from 10% to 90% of the signal maximum) is 3.4 ms, while the decaying part (from 90% to 30% of the signal maximum) is 19 ms. These time constants are typical for NTD-Ge-instrumented macro-bolometers (e.g. comparable results for similar-size bolometers [38, 27]). As illustrated in Fig. 2, the Ge LD exhibits a shorter pulse profile thanks to 120 the smaller heat capacity of both the absorber and the sensor as compared to $\text{Li}_2\text{WO}_4(\text{Mo})$ detector (e.g. see in [24]). However, the Ge LD time response is also limited by the slow response of the NTD Ge thermistor used to read out the heat signal. In spite of that, the observed time profile of the $\text{Li}_2\text{WO}_4(\text{Mo})$ scintillating bolometer signals and the measured counting rate (0.27 counts/s) 125 are compatible with a reasonably low probability of pile-ups ($\sim 5\%$) in a time window (0.2 s) covering a pre-trigger, i.e. a baseline, and a signal.

The sensitivity of the $\text{Li}_2\text{WO}_4(\text{Mo})$ detector, defined as the average pulse height for a 1 keV energy deposit, was measured to be 91.5 nV/keV, in agreement with what is usually observed for such kind of detectors (in particular, for 130 similar-size bolometers tested in the same set-up [38, 27]). By applying a 23 V bias to the electrodes, the LD signal amplitude was amplified to 3.2 $\mu\text{V}/\text{keV}$, which is a factor of 7 larger than the signals read out without an electric field

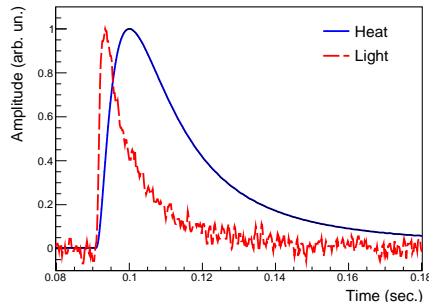


Figure 2: An example of a heat signal from the 8-g $\text{Li}_2\text{WO}_4(\text{Mo})$ bolometer and a corresponding light signal detected by the 1.4-g Ge cryogenic light detector. Both pulses are normalized with respect to their amplitude maximum.

applied on the electrodes. It is worth to be noted that the sensitivity of both detectors (and thus the signal-to-noise ratio) can also be enhanced by optimizing
 135 the thermal sensor design, e.g. as it was done for Ge bolometers [39, 40].

3.2. Energy response

The $\text{Li}_2\text{WO}_4(\text{Mo})$ detector energy response was calibrated and studied in a 113-h long background measurement at 20 mK, using the environmental γ radioactivity (mainly originating from ^{226}Ra and its daughters, ^{214}Pb and ^{214}Bi)
 140 inside the Pb-shielded cryostat. As illustrated by the left panel of Fig. 3, the acquired background energy spectrum shows several peaks below 700 keV and clearly demonstrates that the $\text{Li}_2\text{WO}_4(\text{Mo})$ cryogenic detector provides excellent energy resolution. In particular, the energy resolution of the different γ peaks varies from 2.5(2) keV FWHM at 186 keV (γ following the α decay of ^{226}Ra) to
 145 3.7(1) keV FWHM at 609 keV (γ following the β decay of ^{214}Bi). The baseline noise energy resolution was measured to 1.1(1) keV FWHM. The small difference between the quoted energy resolution and the baseline noise fluctuations indicates a low thermalization noise, already observed for similar detector materials such as lithium molybdate [24] and lithium magnesium molybdate [26].
 150 Thus, the present high spectrometric performance of the $\text{Li}_2\text{WO}_4(\text{Mo})$ bolometric detector can even be improved by operating the detector in conditions

characterized by a lower noise and/or lower counting rate (improved shielding or underground operation).

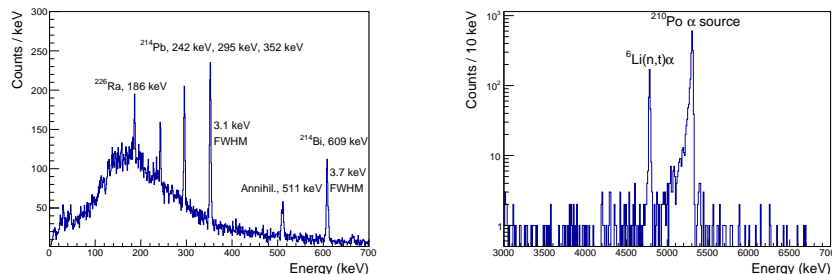


Figure 3: The background energy spectrum accumulated over 113 h with the 8-g $\text{Li}_2\text{WO}_4(\text{Mo})$ bolometric detector operated at 20 mK, and shown over two energy regions. (Left) The low energy part of the $\gamma(\beta)$ distribution up to 700 keV. (Right) The high energy region where decays of α -active radionuclides from U/Th chain are expected to contribute. Alpha particles from the ^{210}Po source and $\alpha + \text{triton}$ events from ambient neutron capture on ^6Li are also visible. The events selection was done using the scintillation light assisted particle identification capability of the $\text{Li}_2\text{WO}_4(\text{Mo})$ bolometric detector (see Sec.3.3 for further details).

The small detector size and the relatively short exposure prevent a detailed
 155 investigation of the detector energy resolution with γ quanta populating the
 MeV energy range. The two prominent populations around 4.8 and 5.3 MeV⁴,
 visible in the right panel of Fig. 3 in the α event region, provide only a provi-
 sional estimate of the detector energy resolution in this energy interval. Indeed,
 the energy of the α particles emitted by the external ^{210}Po source is smeared,
 160 giving rise to an exponential tail of events along the left side of the distribution,
 enlarging its FWHM to 23(1) keV. As opposed to the ^{210}Po α events, the en-
 ergy resolution of the alpha+triton events coming from the $^6\text{Li}(n, t)\alpha$ reaction
 on ambient neutrons is 17(1) keV FWHM since such events take place directly

⁴In the energy scale calibrated with γ quanta, these peaks are shifted by $\sim 3.5\%$ with respect to a nominal energy of the reaction (4784 keV for $^6\text{Li}(n, t)\alpha$ and 5304 keV for ^{210}Po α decay). This effect corresponds to the so-called thermal quenching and it is typical for scintillator-based bolometers on the level of few-ten percent (e.g. see [41, 24]).

within the detector medium. However, the width of the alpha+triton event
165 distribution is affected by surface escapes of the produced particles resulting
thus in a partial energy deposition, and hence an underestimate of the detector
energy resolution (e.g. as it is illustrated in [26]).

3.3. Particle identification capability

Scintillation light assisted particle identification is one of the most important
170 features of scintillating bolometers as it allows an active background rejection
[33]. In addition, selecting α particles from $\gamma(\beta)$ events with high efficiency is
also important in view of the possibility to tag and reconstruct neutron events
coming from the ${}^6\text{Li}(n, t)\alpha$ reaction. This feature would especially be useful
when running a CE ν NS bolometric detector in aboveground conditions, where
175 the muon-induced neutron background is expected to play a decisive role. Such
type of particle identification relies on the fact that the amount of scintilla-
tion light produced by a highly ionizing particle is lower (quenched) than the
scintillation light produced by an electron of the same energy (see e.g. [42]).
In particular, the quenching factor for alpha particles is observed to be at the
180 level of 0.1–0.2 for different crystal scintillators [42, 43, 33]. Thus, a commonly
used parameter, which characterizes the ability of a scintillating bolometer for
particle identification, is the scintillation light yield $LY_{\gamma/(\beta)}$, which is defined
as the ratio of the light signal to the heat signal, both originating from the
energy deposition of a γ/β particle. The scintillation light yield is typically ex-
185 pressed in keV/MeV, and it depends on the combination of several experimental
parameters such as the crystal optical properties (i.e. scintillation efficiency at
low temperatures, light transparency, shape and surface treatment) and the
performance of a photodetector in terms of light collection and detection. For
example, the baseline noise fluctuations of a bolometric photodetector can play
190 a crucial role for particle identification (see, e.g., in [33]).

The left panel of Fig. 4 depicts the light yield distribution of events acquired
during the 113-h background run. The measured light yield is 0.17(1) keV/MeV
and is rather low in comparison to other Li-, Mo-, or W-containing scintillating

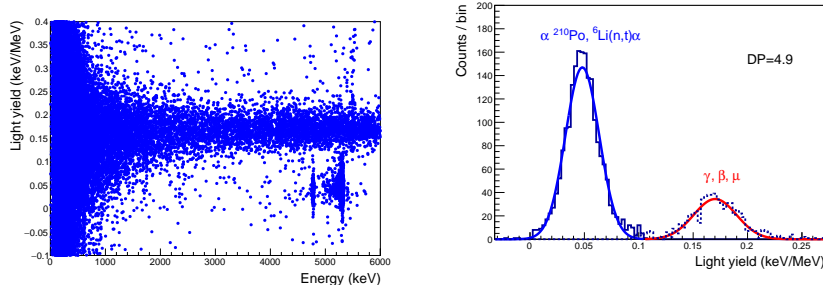


Figure 4: (Left) Light yield versus heat energy scatter plot measured with the 8-g $\text{Li}_2\text{WO}_4(\text{Mo})$ bolometric detector. A 23 V bias was applied on the Ge LD electrodes. (Right) Distribution of the light yield parameter for events with energies between 4.5 and 5.5 MeV: the solid histogram shows α events, which are well separated from the γ/β event distribution represented by the dashed histogram. The achieved discrimination power amounts to 4.87(4) (see text for further details).

bolometers [33], in particular with respect to the (0.7–1.0) keV/MeV measured
 195 light yield for Li_2MoO_4 bolometers. However, the scintillation light collection
 was not optimized, especially because neither reflecting materials on the internal
 lateral side of the Cu holder [25] nor antireflecting SiO coating of the LD used
 from the batch of such devices [34] were used in the tested setup. Thus, the
 light yield of the material is rather expected to be at the level of 0.4 keV/MeV
 200 or more⁵, which is well-enough for a highly efficient $\alpha/\gamma(\beta)$ separation using
 scintillating crystal equipped with NTD-instrumented Ge LD [25]. As demon-
 strated in earlier studies, the use of the Neganov-Trofimov-Luke amplification
 can further enhance the particle identification power of such a setup [34, 33].
 Indeed, having a $LY_{\gamma(\beta)}$ equal to 0.17(1) keV/MeV and the LD baseline noise of
 205 0.3 keV at 0 V electrode bias, a partial $\alpha/\gamma(\beta)$ separation with a discrimina-
 tion power⁶ (DP) of 1.3 was achieved. It was evaluated from the distribution of

⁵For instance, the light yield ~ 0.6 keV/MeV has been recently measured with another $\text{Li}_2\text{WO}_4(\text{Mo})$ bolometer (based on $\varnothing 25 \times 25$ mm crystal produced at NIIC, Novosibirsk) in a low temperature test at CSNSM.

⁶The discrimination power between two Gaussian distributions is calculated as the differ-

^{210}Po α events and from muon-induced events with similar energies. As shown by the right panel of Fig. 4, applying a 23 V bias on the Neganov-Trofimov-Luke light detector electrodes notably amplifies the scintillation signal, resulting in a DP of 4.87(4) or around 5σ (see [24] for further details). A Gaussian fit to the α and the γ/β light yield distributions gives a quenching factor of 0.282(2) for α particles.

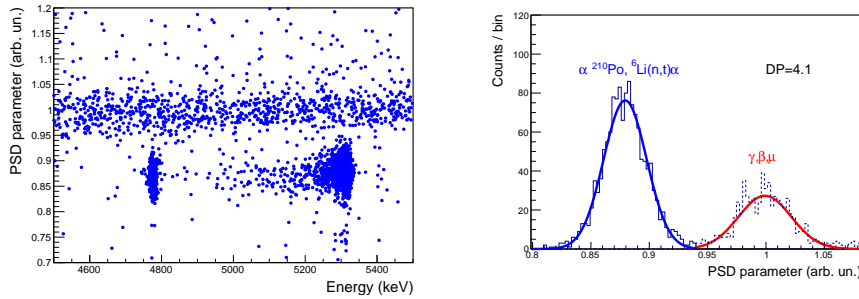


Figure 5: A two-dimensional histogram showing the energy dependence of the PSD parameter (left) and its projected distribution (right) in the 4.5–5.5 MeV energy region, for events detected by the 8-g $\text{Li}_2\text{WO}_4(\text{Mo})$ scintillating bolometer in the 113-h background run. The band of β -, γ - and μ -induced events is clearly separated from the population of alpha+triton events coming from thermal neutron capture on ^6Li ($Q \sim 4.8$ MeV) and from α particles emitted by the ^{210}Po source ($Q \sim 5.3$ MeV). The achieved $\alpha/\gamma(\beta)$ separation, expressed as a discrimination power, is $\text{DP} = 4.11(5)$.

An efficient $\alpha/\gamma(\beta)$ separation can also be achieved with a pulse-shape analysis using only the $\text{Li}_2\text{WO}_4(\text{Mo})$ bolometric signals, as illustrated in Fig. 5. In this particular case, a pulse-shape discrimination (PSD) parameter is defined as the slope of a linear fit to a vector which matches an analyzed heat signal and an average pulse (used in the optimum filter) scaled to the signal maximum height [44]. This PSD parameter allows to achieve a slightly better separation power than e.g. using another simple PSD parameter as the rise and decay times, demonstrating that a more complex PSD parameter can even improve

ence between their mean values scaled by the square root of the sum of squared standard deviations.

the particle identification capability of the $\text{Li}_2\text{WO}_4(\text{Mo})$ bolometric detector. With the present level of the PSD-based $\alpha/\gamma(\beta)$ discrimination power, $\text{DP} = 4.11(5)$, more than 99.9% of $\gamma(\beta)$ events can be rejected from the region of interest, which is definitely a very useful ability for performing neutron tagging and spectroscopy exploiting the pulse-shape analysis.

3.4. Crystal radiopurity

Ensuring low levels of radioactive contaminants can be of paramount importance when using a $\text{Li}_2\text{WO}_4(\text{Mo})$ -based bolometric device both for the $\text{CE}\nu\text{NS}$ detection at reactors and for the spectroscopy of neutrons. The expected $\text{CE}\nu\text{NS}$ recoil signal from reactor $\bar{\nu}_e$ in $\text{Li}_2\text{WO}_4(\text{Mo})$ is expected to be below 1 keV, hence requiring a detailed understanding and a tight control of the backgrounds in this region. As concerns the neutron spectroscopy application, $(\alpha+t)$ events lie at 4.8 MeV (thermal neutrons) and above (fast neutrons), which should hence not be polluted by α energy deposits coming from the U and Th decay chains. Finally, applying high radiopurity standards for the fabrication of $\text{Li}_2\text{WO}_4(\text{Mo})$ crystals could also help in reducing the total counting rate, which is important when running cryogenic detectors in aboveground conditions since they are known to be slow devices.

The elemental composition of the $\text{Li}_2\text{WO}_4(\text{Mo})$ material does not contain radioactive nuclides⁷. Therefore, the radioactive impurity content of the $\text{Li}_2\text{WO}_4(\text{Mo})$ crystal should mostly be driven by the purity of the initial materials and by the cleanliness of the equipment used to fabricate the crystal. The chemical affinity between lithium and potassium can lead to a ^{40}K activity in Li-containing materials at the level of ~ 0.1 Bq/kg. It can be mitigated by the selection of radiopure Li-containing powder and/or by applying additional purification processes [24]. This contamination is also expected to be present in the studied $\text{Li}_2\text{WO}_4(\text{Mo})$

⁷The activity of ^{180}W alpha decay and ^{100}Mo double-beta decay, present in tungsten and molybdenum isotopic composition respectively, is negligible because of their low amount in the studied material and extremely long half-lives ($\sim 10^{18}$ yr).

crystal. However, in our test the determination of ^{40}K activity at the level of hundreds of mBq/kg or lower is impossible in an aboveground bolometric test. For example, aboveground [23] and underground [24] measurements of the same Li_2MoO_4 bolometric detector resulted in very different sensitivities to its radiopurity level. The $\text{Li}_2\text{WO}_4(\text{Mo})$ contamination by radioactive nuclides from the U/Th chains can be investigated in the present data thanks to the achieved efficient $\alpha/\gamma(\beta)$ separation, allowing to select α particles with energies in the 4 to 7 MeV range, as expected from the α decays of $^{238}\text{U}/^{232}\text{Th}$ and their daughters. The energy spectrum of α particles, shown in the right panel of Fig. 3, does not contain any other peculiarities except those caused by thermal neutron capture on ^6Li and by the ^{210}Po source, as well as a hint on a bulk ^{210}Po contamination (a peak-like structure around 5.4 MeV with an activity 4.2(12) mBq/kg). Using the approach described in details in [45], upper limits at the 90% confidence level on the bulk contamination of the $\text{Li}_2\text{WO}_4(\text{Mo})$ crystal can be estimated: ≤ 0.8 mBq/kg of ^{232}Th , ≤ 1.0 mBq/kg of ^{228}Th , ≤ 3.4 mBq/kg of ^{238}U and ≤ 2.1 mBq/kg of ^{226}Ra . These results indicate a low U/Th content, and can be considerably improved by increasing the measurement exposure. If necessary, $\mu\text{Bq/kg}$ -level sensitivities in U/Th content of $\text{Li}_2\text{WO}_4(\text{Mo})$ crystals could also be achieved benefiting from the recent progress in the development of lithium molybdate crystals [24, 46, 25].

4. Conclusions and perspectives

In the perspective of a precise measurement of CE ν NS close to a reactor facility, this article reports on the first test of a lithium tungstate cryogenic detector developed in the framework of the BASKET R&D program. The choice of lithium tungstate as an absorber material was driven by two main reasons: the presence of a heavy element to enhance the CE ν NS rate and the presence of ^6Li to leverage the $^6\text{Li}(n,t)\alpha$ reaction for neutron background identification and/or mitigation. In this context, a Mo-doped lithium tungstate crystal ($\text{Li}_2\text{Mo}_{0.08}\text{W}_{0.92}\text{O}_4$) with a size of $\varnothing 18 \times 7$ mm and a mass of 8 g was investigated

for the first time as a low temperature detector.

The $\text{Li}_2\text{WO}_4(\text{Mo})$ scintillating bolometer was operated at a 20 mK (sample holder) temperature in a pulse-tube-based $^3\text{He}/^4\text{He}$ dilution refrigerator running in an aboveground laboratory at CSNSM (Orsay, France). The time constants of the bolometric signals (respectively rise and decay time parameters) were measured to be in the 1–10 ms range, and are in agreement with what is usually observed for the NTD Ge thermistor technology. The obtained baseline noise (1.1 keV FWHM) is similar to values reported for other macro bolometers tested in the same set-up. The $\text{Li}_2\text{WO}_4(\text{Mo})$ detector baseline noise was not meant to be optimized, and can be further improved by operating the detector in low noise conditions and/or by adjusting the temperature sensor to enhance the bolometer sensitivity. The tested $\text{Li}_2\text{WO}_4(\text{Mo})$ bolometric detector showed an excellent energy resolution (e.g. 3.7 keV FWHM at 609 keV γ quanta). It also exhibited a low light yield value of 0.17 keV/MeV, which is a factor 3–4 smaller than that usually observed for example in Li_2MoO_4 cryogenic detectors. The poor light collection did not prevent to investigate the scintillation light assisted particle identification capability of $\text{Li}_2\text{WO}_4(\text{Mo})$. Exploiting a thin Ge ($\varnothing 44 \times 0.175$ mm) bolometer with the Neganov-Trofimov-Luke signal amplification, a 5σ separation of $\beta/\gamma/\mu$ both from neutron-induced events ($\alpha+t$) and from α particles of a ^{210}Po source was demonstrated. Similar particle separation (4σ) was achieved by using a pulse-shape analysis on the $\text{Li}_2\text{WO}_4(\text{Mo})$ bolometric signals. Finally, the energy spectrum of α particles did not show any hint on a bulk contamination from U/Th α -active radionuclides (except ^{210}Po with a 4.2(12) mBq/kg activity), thus resulting to upper limits on their activity at the level of (0.8–3.4) mBq/kg. More precise investigations of the crystal radiopurity require an underground operation.

All these results confirm the promising potential of lithium tungstate-based bolometric detectors for the study of $\text{CE}\nu\text{NS}$ in nearly aboveground conditions, such as those met at a reactor facility. Thanks to their neutron tagging capabilities and their heavy element content, $\text{Li}_2\text{WO}_4(\text{Mo})$ cryogenic detectors could either be used as a neutron flux monitoring system, a $\text{CE}\nu\text{NS}$ event detector

and/or an active neutron-absorbing veto. The next steps of the BASKET R&D project therefore consist in testing of $\text{Li}_2\text{WO}_4(\text{Mo})$ materials obtained with different production processes (different compound synthesis, advanced crystal
310 growth method) together with the use of different phonon sensor technologies (e.g. metallic magnetic calorimeters or high impedance NbSi transition-edge sensors) targeting for a detector prototype with a fast time response, $O(100 \mu\text{s}$ rise time), and a very low energy threshold ($\lesssim 50$ eV). Moreover, the development of a ^6Li -enriched $\text{Li}_2\text{WO}_4(\text{Mo})$ crystal is in progress. The use of
315 ^6Li -enriched crystals will significantly enhance the probability of a neutron capture inside the material, and will then improve the neutron identification and spectroscopy capabilities of $\text{Li}_2\text{WO}_4(\text{Mo})$ -based bolometric detectors, which is rather important in context of its application for the $\text{CE}\nu\text{NS}$ detection.

Acknowledgements

320 We acknowledge the financial support of the Cross-Disciplinary Program on Instrumentation and Detection of CEA, the French Alternative Energies and Atomic Energy Commission. This work has been partially funded by the P2IO LabEx (ANR-10-LABX-0038) in the framework of "Investissements d'Avenir" (ANR-11-IDEX-0003-01) managed by the French National Research Agency
325 (ANR). I.Ch. Avetissov was supported by the project of the Ministry of Science and High Education of the Russian Federation (the grant RFMEFI57418X0186). The work of F.A. Danevich and V.I. Tretyak was supported in part by the IDEATE International Associated Laboratory (LIA) and by the program of the National Academy of Sciences of Ukraine Fundamental research on high-energy
330 and nuclear physics (International cooperation).

References

- [1] D. Z. Freedman, Coherent effects of a weak neutral current, Phys. Rev. D 9 (1974) 1389. doi:10.1103/PhysRevD.9.1389.

- [2] D. Akimov, et al., Observation of coherent elastic neutrino-nucleus scattering, *Science* 357 (2017) 1123. doi:10.1126/science.aao0990.
- [3] D. Akimov, et al., COHERENT Collaboration data release from the first observation of coherent elastic neutrino-nucleus scattering, arXiv:1804.09459doi:10.5281/zenodo.1228631.
- [4] The Magnificent CE ν NS Workshop, University of Chicago, Chicago, IL USA, <https://kicp-workshops.uchicago.edu/2018-CEvNS/> (2018).
- [5] M. Lindner, W. Rodejohann, X. Xu, Coherent Neutrino-Nucleus Scattering and new Neutrino Interactions, *JHEP* 03 (2017) 097. arXiv:1612.04150, doi:10.1007/JHEP03(2017)097.
- [6] D. K. Papoulias, T. S. Kosmas, COHERENT constraints to conventional and exotic neutrino physics, *Phys. Rev. D* 97 (3) (2018) 033003. arXiv:1711.09773, doi:10.1103/PhysRevD.97.033003.
- [7] J. Billard, J. Johnston, B. J. Kavanagh, Prospects for exploring New Physics in Coherent Elastic Neutrino-Nucleus Scattering, *JCAP* 11 (2018) 016.
- [8] M. Cadeddu, C. Giunti, Y. F. Li, Y. Y. Zhang, Average CsI neutron density distribution from COHERENT data, *Phys. Rev. Lett.* 120 (7) (2018) 072501. arXiv:1710.02730, doi:10.1103/PhysRevLett.120.072501.
- [9] A. Aguilar-Arevalo, et al., Results of the Engineering Run of the Coherent Neutrino Nucleus Interaction Experiment (CONNIE), *JINST* 11 (07) (2016) P07024. arXiv:1604.01343, doi:10.1088/1748-0221/11/07/P07024.
- [10] G. Agnolet, et al., Background Studies for the MINER Coherent Neutrino Scattering Reactor Experiment, *Nucl. Instrum. Meth. A* 853 (2017) 53–60. arXiv:1609.02066, doi:10.1016/j.nima.2017.02.024.

- 360 [11] J. Billard, et al., Coherent Neutrino Scattering with Low Temperature Bolometers at Chooz Reactor Complex, *J. Phys. G* 44 (2017) 105101. [arXiv:1612.09035](#), [doi:10.1088/1361-6471/aa83d0](#).
- [12] J. Hakenmüller, et al., Neutron-induced background in the CONUS experiment [arXiv:1903.09269](#).
- 365 [13] R. Strauss, et al., The ν -cleus experiment: A gram-scale fiducial-volume cryogenic detector for the first detection of coherent neutrino-nucleus scattering, *Eur. Phys. J. C* 77 (2017) 506. [arXiv:1704.04320](#), [doi:10.1140/epjc/s10052-017-5068-2](#).
- [14] G. Angloher, et al., Exploring CEvNS with NUCLEUS at the Chooz Nuclear Power Plant, [arXiv:1905.10258](#).
- 370 [15] <http://irfu.cea.fr/Phoceae/Page/index.php?id=861>.
- [16] J. Meija, et al., Isotopic compositions of the elements 2013 (IUPAC Technical Report), Vol. 88, 2016.
- [17] A. R. Putra, Y. Tachibana, M. Tanaka, T. Suzuki, Lithium isotope separation using displacement chromatography by cation exchange resin with high degree of cross-linkage, *Fusion Engineering and Design* 136 (2018) 377.
- 375 [18] M. B. Chadwick, et al., ENDF/B-VII.1 Nuclear Data for Science and Technology: Cross Sections, Covariances, Fission Product Yields and Decay Data, *Nucl. Data Sheets* 112 (2011) 2887.
- [19] P. de Marcillac, et al., Characterization of a 2 g LiF bolometer, *Nucl. Instr. Meth. A* 337 (1993) 95.
- 380 [20] J. Gironnet, et al., Neutron spectroscopy with ^6LiF bolometers, *AIP Conf. Proc.* 1185 (2009) 751.
- [21] M. Martinez, et al., Scintillating bolometers for fast neutron spectroscopy in rare events searches, *J. Phys.: Conf. Ser.* 375 (2012) 012025.
- 385

- [22] L. Cardani, et al., Development of a Li_2MoO_4 scintillating bolometer for low background physics, *JINST* 8 (2013) P10002.
- [23] T. Bekker, et al., Aboveground test of an advanced Li_2MoO_4 scintillating bolometer to search for neutrinoless double beta decay of ^{100}Mo , *Astropart. Phys.* 72 (2016) 38.
- 390 [24] E. Armengaud, et al., Development of ^{100}Mo -containing scintillating bolometers for a high-sensitivity neutrinoless double-beta decay search, *Eur. Phys. J. C* 77 (2017) 785.
- [25] D. V. Poda, et al., ^{100}Mo -enriched Li_2MoO_4 scintillating bolometers for $0\nu 2\beta$ decay search: from LUMINEU to CUPID-0/Mo projects, *AIP Conf. Proc.* 1894 (2017) 020017.
- 395 [26] F. A. Danevich, et al., Growth and characterization of a $\text{Li}_2\text{Mg}_2(\text{MoO}_4)_3$ scintillating bolometer, *Nucl. Inst. Meth. A* 889 (2018) 89.
- [27] G. Buşe, et al., First scintillating bolometer tests of a CLYMENE R&D on Li_2MoO_4 scintillators towards a large-scale double-beta decay experiment, *Nucl. Instr. Meth. A* 891 (2018) 87.
- 400 [28] O. Barinova, et al., Solid solution $\text{Li}_2\text{MoO}_4 - \text{Li}_2\text{WO}_4$ crystal growth and characterization, *J. Crystal Growth* 468 (2017) 365. doi:10.1016/j.jcrysgro.2016.10.009.
- [29] D. M. Chernyak, et al., Effect of tungsten doping on ZnMoO_4 scintillating bolometer performance, *Optical Materials* 49 (2015) 67.
- 405 [30] E. E. Haller, Advanced far-infrared detectors, *Infrared Phys. Techn.* 35 (1994) 127.
- [31] E. Andreotti, et al., Production, characterization and selection of the heating elements for the response stabilization of the CUORE bolometers, *Nucl. Instrum. Meth. A* 664 (2012) 161.
- 410

- [32] A. Alessandrello, et al., Methods for response stabilization in bolometers for rare decays, *J. Crystal Growth* 412 (1998) 454.
- [33] D. Poda, A. Giuliani, Low background techniques in bolometers for double-beta decay search, *Int. J. Mod. Phys. A* 32 (2017) 1743012.
- [34] V. Novati, et al., Charge-to-heat transducers exploiting the Neganov-Trofimov-Luke effect for light detection in rare-event searches, *Nucl. Instrum. Meth. A* 940 (2019) 320.
- [35] M. Mancuso, et al., An aboveground pulse-tube-based bolometric test facility for the validation of the LUMINEU ZnMoO_4 crystals, *J. Low Temp. Phys.* 176 (2014) 571.
- [36] C. Arnaboldi, et al., The programmable front-end system for CUORICINO, an array of large mass bolometers, *IEEE Trans. Nucl. Sci.* 49 (2002) 2440.
- [37] E. Gatti, P. Manfredi, Processing the signals from solid-state detectors in elementary-particle physics, *Riv. Nuovo Cim.* 9 (1986) 1.
- [38] A. S. Barabash, et al., First test of an enriched $^{116}\text{CdWO}_4$ scintillating bolometer for neutrinoless double-beta-decay searches, *Eur. Phys. J. C* 76 (2016) 487.
- [39] J. Billard, M. De Jesus, A. Juillard, E. Queguiner, Characterization and Optimization of EDELWEISS-III FID800 Heat Signals, *J. Low Temp. Phys.* 184 (2016) 299.
- [40] E. Armengaud, et al., Searching for low-mass dark matter particles with a massive Ge bolometer operated above ground, *Phys. Rev. D* 99 (2019) 082003.
- [41] C. Arnaboldi, et al., CdWO_4 scintillating bolometer for Double Beta Decay: Light and heat anticorrelation, light yield and quenching factors, *Astropart. Phys.* 34 (2010) 143.

- [42] V. I. Tretyak, Semi-empirical calculation of quenching factors for ions in scintillators, *Astropart. Phys.* 33 (2010) 40.
- 440 [43] V. I. Tretyak, Semi-empirical calculation of quenching factors for scintillators: new results, *EPJ Web of Conferences* 65 (2014) 02002.
- [44] I. C. Bandac, et al., The $0\nu 2\beta$ -decay CROSS experiment: preliminary results and prospects, Submitted to *JHEP* [arXiv:1906.10233](https://arxiv.org/abs/1906.10233).
- [45] E. Armengaud, et al., Development and underground test of radiopure
445 ZnMoO_4 scintillating bolometers for the LUMINEU $0\nu 2\beta$ project, *JINST* 10 (2015) P05007.
- [46] V. D. Grigorieva, et al., Li_2MoO_4 crystals grown by low thermal gradient Czochralski technique, *J. Mat. Sci. Eng. B* 7 (2017) 63.